Biochimica et Biophysica Acta 807 (1985) 35–43
Elsevier

BBA 41716

Photosystem I reaction center from *Mastigocladus laminosus*. Correlation between reduction state of the iron-sulfur centers and the triplet formation mechanisms

Rachel Nechushtai [a], Nathan Nelson [a], Oded Gonen [b] and Haim Levanon [b,*]

[a] *Department of Biology, Technion-Israel Institute of Technology, Haifa 32000 and* [b] *Department of Physical Chemistry and the Fritz Haber Research Center for Molecular Dynamics, The Hebrew University of Jerusalem, Jerusalem 91904 (Israel)*

(Received February 29th, 1984)

Key words: Photosystem I; Reaction center; Triplet state; ESR; Iron-sulfur center; (*Mastigocladus* sp.)

EPR study of reduced ground and photoexcited triplet state of Photosystem I reaction center in the thermophylic cyanobacterium *Mastigocladus laminosus* at 8 K is reported. In the reduced ground state preparation, the iron-sulfur EPR spectra are found to be similar to that of Photosystem I reaction center of higher plants. Two types of transient photoexcited triplets are observed and are correlated to the reduction state of the iron-sulfur centers. When electrons can be transferred freely through the acceptors chain, a polarized triplet spectrum is observed, typical of spin-orbit intersystem crossing mechanism with lifetime of approx. 2 ms and is attributed to chlorophyll *a*, either at the antenna or at A_1 in the electron-transport chain. When the iron-sulfur centers are reduced the triplet spectrum is typical of a radical-pair intersystem crossing mechanism with triplet lifetime shorter than 1 ms, and is attributed to P-700. Both species have similar spectroscopic zero field splitting parameters identifying both as chlorophyll *a*.

Introduction

The primary photoevent occurring in PS-I reaction centers results in charge separation and successive electron-transfer processes to reduce bound ferredoxins in the electron-transport chain. While in various higher plants the PS-I reaction center consists of seven different subunits [1–4], this complex in green alga contains only four subunits [5].

Recently, PS-I reaction center was isolated from two species of cyanobacteria [6,7], the complex purified from the thermophylic cyanobacterium *Mastigocladus laminosus* [7] contained four different subunits with molecular weights of 70000 (subunit I), 16000 (subunit II), 11000 (subunit III), and 10000 (subunit IV). The purified reaction center was active in cytochrome *c* photooxidation with a temperature optimum of 60°C. Its subunit I was found to be similar in molecular weight, P-700 content and pattern of appearance in SDS gels to subunits I from higher plants and green alga PS-I reaction center. Immunological cross reactivity between subunits I of higher plants, green alga and cyanobacterium reaction centers was detected [7].

P-700 was identified as the electron donor of the PS-I reaction center [8] and upon illumination electrons are transferred to the primary electron acceptor A_1 [9–11] * from which the electrons are further transferred to the iron-sulfur centers A_2 (X), A_3 (B) and A_4 (A) [12]. The presence of

Abbreviations: PS I, Photosystem I; Chl *a*, chlorophyll *a*; Mes, 4-morpholineethanesulphonic acid; MTHF, methyltetrahydrofuran.

* A_1 in this context refers to Chl-*a* species immediately following P-700 in the electron-transport chain. The experimental data do not disclose detailed information as to the participation of an earlier primary acceptor A_0 (see Ref. 11).

bound ferredoxins was found in preparations enriched in PS I from various sources [13–20], including preparations of higher plants PS-I reaction center consisting of either seven [21] or eleven [22] subunits.

Since the *Mastigocladus* PS-I reaction center consists of four subunits only, a functional equivalency to the PS-I reaction center of higher plants has been sought for in this study by EPR spectroscopy. Two paramagnetic species of PS-I reaction center are discussed in the present work:
(1) bound ferredoxins in the reduced ground state and
(2) the photoexcited triplet state. The ability to detect the iron-sulfur complex lends support to the determination of existence of such functional equivalency between PS-I reaction center of *Mastigocladus* and higher plants.

EPR triplet detection may provide an insight on the molecular structure and coupling mechanism between the photoexcited singlet and triplet manifolds. Light modulation EPR spectroscopy monitoring the photoexcited triplet state is a convenient tool to study the spin dynamics associated with this state. This method has been applied to many in vitro systems [23–25] as well as in vivo preparations [20,22–27,35]. In all cases studied previously and are relevant to the present work, the triplet spectra exhibit anomalous lineshape due to selective intersystem crossing routes from the photoexcited singlet to the triplet state. This phenomenon is commonly termed as electron spin polarization (ESP). For recent reviews and relevant references on EPR triplet detection, see for instance Refs. 23, 24 and 25.

Two mechanisms of intersystem crossing (triplet ← singlet) are known to be responsible for the observed EPR triplet lineshape and the associated spin dynamics. The most common one in in vitro systems is the so-called spin-orbit intersystem crossing, and the one often observed in in vivo systems is the radical-pair intersystem crossing [23–25]. Although both mechanisms give rise to EPR detectable triplet states, the lineshape in term of the polarization patterns is fundamentally different.

In the spin-orbit intersystem crossing, the selective population of the triplet sublevels in high magnetic field will result in polarization patterns which are governed by the nature of the singlet-triplet mixing. In this case selective intersystem crossing occurs, at high magnetic fields, to substates T_0, $T_{\pm 1}$ and the high-field populations are given by Eqn. 1:

$$N_{\pm 1} \approx \tfrac{1}{2}(N_j + N_k)$$

$$N_0 = N_i \text{ for } \boldsymbol{B} \| i \ (i = X, Y, Z) \tag{1}$$

where X, Y, Z are the canonical orientations and $N_{i,j,k}$ are the zero-field levels population. The polarization directions of the transient triplet spectrum in the fast limit will show one of six patterns determined by the sign of D (the axial zero-field splitting parameter) and the spin sublevels at zero field, selectively populated from the singlet. As an illustration, the polarization pattern of the transitions in the $\Delta M_s = \pm 1$ region for $D > 0$, and selective population of T_Y level is given by:

$$e(Z_2)e(X_1)e(Y_1)a(Y_2)a(X_2)a(Z_1) \tag{2}$$

where e and a are emissive and absorptive lines, respectively. Therefore, under conventional spin orbit intersystem crossing mechanism there is always a change in sign (from e to a for a given set of transitions as defined by each half spectrum p_i, ($p = X, Y, Z$; $i = 1, 2$).

In the radical pair intersystem crossing mechanism, the population of the sublevels is still selective. However, it differs from that discussed above as only the T_0 state is overpopulated regardless of the relative orientation of the principal axes with respect to the external magnetic field $\boldsymbol{B}$. This mechanism occurs in those systems where radical pairs $[\dot{A}^+ \dot{B}^-]$ can be produced following the primary photoexcitation [23–25,28]. The difference in magnetic environment between $\dot{A}^+$ and $\dot{B}^-$ may result in mixing between the photoexcited singlet $M_{s=0} = 0$ and that of the triplet component $M_{s=1} = 0$. This will develop a triplet character in the radical pair, and a back electron transfer will produce $A^T B$ which is EPR detectable. This reaction scheme is:

$$[AB] \xrightarrow{h\nu} [A^*B] \underset{\text{transfer}}{\overset{e^-}{\longleftrightarrow}} [\dot{A}^+ \dot{B}^-]^S$$

$$\xrightarrow[\text{intersystem crossing}]{\text{radical}} [\dot{A}^+ \dot{B}^-]^T \xrightarrow[\text{transfer}]{\text{back } e^-} [A^T B] \tag{3}$$

Under this mechanism the triplet EPR polarization patterns will be:

$$a(Z_2)e(X_1)e(Y_1)a(Y_2)a(X_2)e(Z_1) \quad (4)$$

This pattern is markedly different from Eqn. 2 as here, there is no change in the sign (from *e* to *a* or vice versa) for a given set of transition (each half spectrum). It should be clear from the above argumentation that once a polarized spectrum is obtained, it is possible to determine from the polarization patterns which intersystem crossing mechanism prevailed.

In the present work we report on the detection of the iron-sulfur centers in *Mastigocladus laminosus* PS-I reaction center which contains only four subunits and compare it to the EPR spectrum of spinach which contains seven such subunits, typical of higher plants. When photoexcited, *Mastigocladus* PS-I reaction center displays two different triplet EPR spectra which are associated with two different pathways for the intersystem crossing, namely the spin-orbit and radical-pair mechanisms. It is found that the choice of which mechanism predominates (and subsequently which species is observed) depends on the reduction state of the iron-sulfur centers.

Materials and Methods

Analytical methods

Chlorophyll was measured according to Arnon [29] and P-700 was detected as previously described [1,2]. Gel electrophoresis in slab gels containing an exponential gradient of 10–15% acrylamide was also performed [30].

Growing of cells and isolation of PS-I reaction center

Mastigocladus laminosus was grown in medium D of Castenholz [31] at pH 8.2, with constant stirring at 50°C [32,33]. The cultures were bubbled with water saturated air supplemented with 5% CO_2. The cells were illuminated with white light at an intensity of about 10^2 J · m^{-2} · s^{-1}. After 4–5 days the cells were harvested by centrifugation at 2000 × *g* for two min. The cells were washed in a buffer containing 10 mM Tris-HCl (pH 8.0) and 10 mM NaCl, and recentrifugated at 2000 × *g* for an additional 2 min. The washed cells were resuspended in the same buffer containing 0.4 M sucrose at Chl *a* concentration of 2 mg/ml. PS-I reaction center was isolated from *Mastigocladus* [7] and from spinach [4] as previously described.

Spinach and Mastigocladus PS-I reaction center preparation for EPR studies

Spinach PS-I reaction center at chlorophyll concentration of 2 mg/ml was suspended in a solution containing 0.1 M glycine (pH 10.1)/0.1% sodium dithionite (w/v)/10 μM methyl viologen and about 50% glycerol. *Mastigocladus* PS-I reaction center with chlorophyll concentration of 2 mg/ml was suspended in a similar solution with a sodium dithionite concentration of 1% (w/v). Samples of 200 μl were transferred to a 4 mm outer diameter quartz tubes and frozen under illumination to the desired experimental temperature. This preparation method results in the reduction of A_2, A_3 and A_4 without affecting the reduction state of A_1 [15,16,19,35]. As expected, freezing these samples in the dark should prohibit the reduction of A_2 [15,16,19,35]. The unblocked samples were prepared in the same buffer (0.1 M glycine, pH 10.1) without sodium dithionite, and frozen in the dark.

Instrumental

The EPR spectrometer used was a Varian E-12, the cryostat was an Air-Products Helitran LTD-3-110, which maintained a temperature of 8 K in all experiments. When photoexcitation was required, an electronically modulated xenon arc (Eimac 150 W) was used and the EPR signal from the 100 kHz lock-in amplifier was fed into a second phase-sensitive detector in reference with the light modulation frequency. A detailed description of the light excitation and signal detection is available elsewhere [34]. The exciting light was passed through a 5 cm water cell and a Corning 3-73 cut-off filter ($\lambda_{pass} > 390$ nm). The experimental results were digitized by a Nicolet Explorer III-A digital oscilloscope interfaced to a microcomputer on line with the experiment, and processed off line on a VAX 11/750.

Results and Discussion

The purified PS-I reaction center isolated from spinach and cyanobacterium *Mastigocladus*

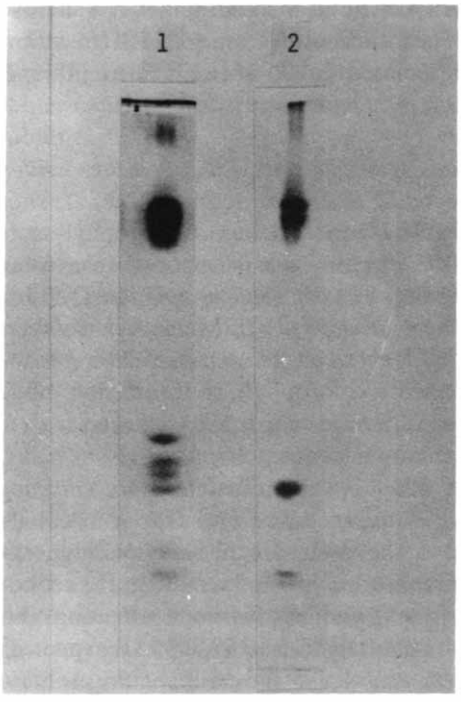

Fig. 1. SDS-polyacrylamide gel patterns of spinach (lane 1) and *Mastigocladus* (lane 2) PS-I reaction center. Preparations obtained as described in the main text were dissociated for about 2 h at room temperature in 2% SDS and 2% β-mercaptoethanol. Samples containing about 15 μg protein were electrophoresed on an exponential 10–15% acrylamide gel.

laminosus contained about 50 Chl *a* molecules per P-700. The polypeptide profiles of the PS-I reaction center purified from spinach and *Mastigocladus* are shown in Fig. 1. While the spinach complex contains seven subunits the *Mastigocladus* PS-I reaction center consists of four only. Subunits I in both preparations were similar in molecular weight (70000), and appearance in the SDS gels. As indicated above, some preparations for the EPR measurements were done at pH 10.1. The results in Fig. 2 show that light-induced absorption change of P-700 can be detected at the high pH as well as at pH 8.0. Although the kinetic trace at pH 10.1 exhibits a lower photooxidation rate constant than that obtained at pH 8.0, it is concluded that PS-I reaction center is still functional under the present experimental conditions.

The presence of the iron-sulfur centers in the two reduced PS-I reaction centers was verified by following their EPR signals. The EPR spectrum of

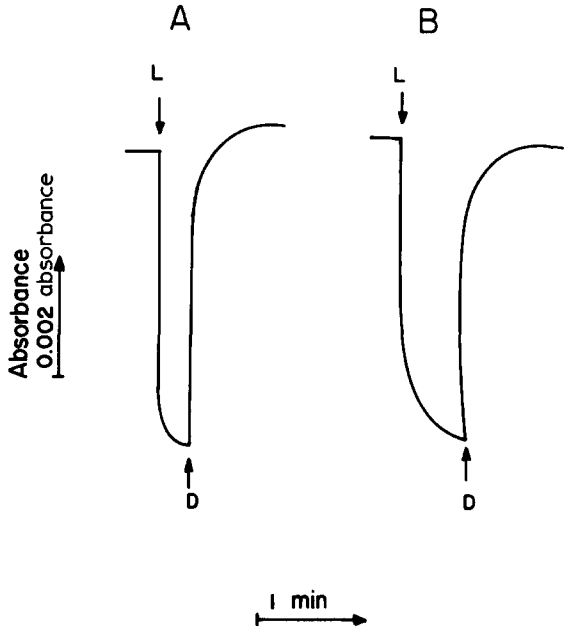

Fig. 2. Photooxidation of P-700 in *Mastigocladus* PS-I reaction center. The reaction mixture contained in a final volume of 1 ml, 20 μmol of Mes-tricine (pH 8.0) (A) or 20 μmol glycine (pH 10.1), (B), 10 nmol sodium ascorbate, 3 μg *N*-methylphenazonium methosulfate and PS-I reaction center equivalent to 17 μg of chlorophyll. Light-induced absorbance changes were recorded at 430 nm as previously described [1,2].

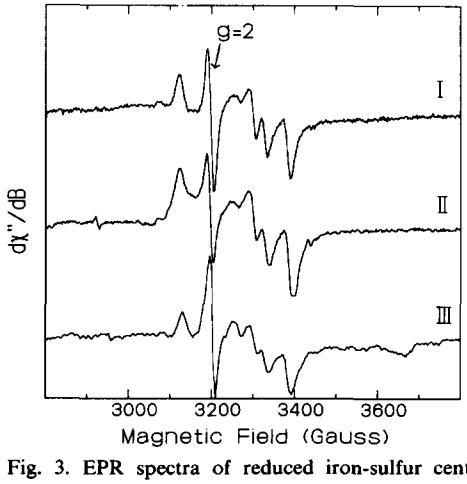

Fig. 3. EPR spectra of reduced iron-sulfur centers in PS-I reaction center isolated from spinach (I) and *Mastigocladus* (II and III). Spectra I and II were recorded after the samples were frozen in the dark (A_3 and A_4 reduced), trace III was recorded after freezing under continuous illumination (A_2, A_3, A_4 reduced). Microwave power and spectrometer gain are 20, 60, and 100 mW and 1600, 2000, and 1600 for I, II and III, respectively. Modulation amplitude of 10 Gauss; scan time, 4 min, time constant, 0.1 s and temperature, 8 K, are common to all spectra.

the four subunit *Mastigocladus* PS-I reaction center at pH 10.1 is given in the lower trace in Fig. 3, and is compared to that of spinach (upper trace). The similarities between the two spectra suggest that both reaction centers are similar with respect to bound ferredoxin content.

Upon illumination of *Mastigocladus* PS-I reaction center, two different transient triplet EPR spectra having different lifetimes are observed depending on the reduction state of the bound ferredoxins (Fig. 4). Each one of those spectra exhibits a typical lineshape, characteristic of a different intersystem crossing mechanism, as reflected by the polarization patterns. When the system is at normal oxidation state (no sodium dithionite, frozen in the dark) trace I in Fig. 4 is obtained and the kinetic behavior is given in Fig. 5. When the iron-sulfur centers are reduced the lower trace II in Fig. 4 results in with kinetics given in Fig. 6.

We interpret these observations in terms of the two intersystem crossing mechanisms described above. In the unblocked system the electrons are free to flow and are being transferred through the complete cycle. The transient EPR spectrum obtained under these conditions, shows a polarization pattern typical of conventional spin orbit intersystem crossing, namely: *

$$a(Z_2)a(X_1)a(Y_1)e(Y_2)e(X_2)e(Z_1) \qquad (5)$$

This is reflected by the change from emission to absorption in each transition. When the iron-sulfur centers are reduced, the spectrum nr. II in Fig. 4 exhibits a polarization pattern:

$$a(Z_2)e(X_1)e(Y_1)a(Y_2)a(X_2)e(Z_1) \qquad (6)$$

with no change in sign of polarization for each transition *, a situation typical to photoexcited

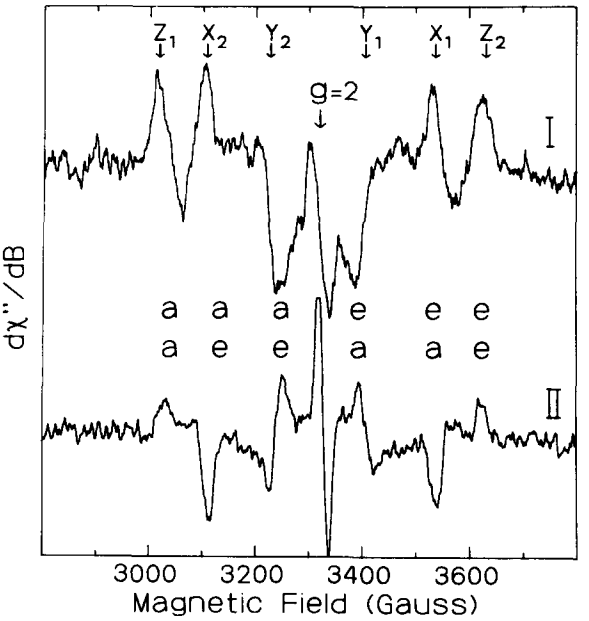

Fig. 4. First harmonic representation $d\chi''/dB$ of photoexcited transient triplet EPR spectra of *Mastigocladus*. The upper trace (I) is of the sample at its normal oxidation state and the lower trace (II) is of the blocked system. The samples were prepared as described in the text. The spectra were recorded at 5 mW power, modulation amplitude, 32 G, temperature, 8 K; light modulation frequency, 500 Hz; scan time, 8 min and time constant, 1 s. The polarization patterns (e = emission, a = absorption) were determined as described in the text *.

triplets observed in the reaction center of bacteria [23–28] and recently in PS-I reaction center of spinach [20,22,35]. These observations are con-

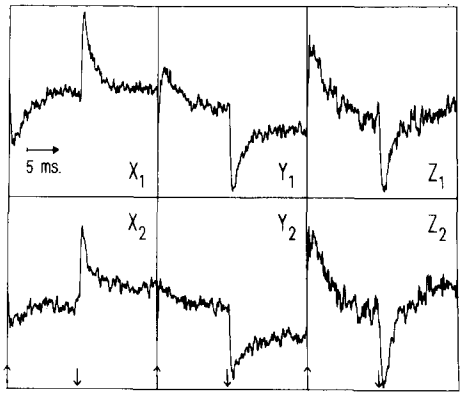

Fig. 5. Kinetic traces of the EPR signal at the canonical fields (see Fig. 4, spectrum I) of unblocked PS-I reaction center of *Mastigocladis*. Light modulation frequency is 50 Hz. ↑, ↓ indicate the driving light pulse on and off time, respectively. Each trace is a computer accumulation of 2500 pulses.

* The polarization patterns indicated were obtained from the derivative line at $g \approx 2$ in both traces of Fig. 4. This line is not attributed to a triplet spectrum but rather to a light-induced radical. It is evident from schemes 7 and 10 that: (a) radicals are constantly present in the PS-I reaction center once the light is on and (b) thermal equilibrium sets in for these radicals within a few microseconds [26,27], well under the EPR time resolution. One may thus conclude that the electron spin in the radical has equilibrated, and represents an absorptive line. The nature of the triplet lines was determined with reference to the signal phase of this radical.

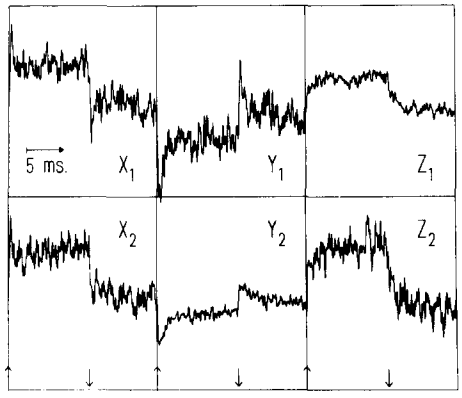

Fig. 6. Kinetic traces of the EPR signal at the canonical fields (see Fig. 4, spectrum II) of PS-I reaction center of *Mastigocladus* where the iron-sulfur centers have been reduced (blocked). Light modulation frequency is 60 Hz, ↑, ↓ indicate the driving light pulse on and off time, respectively. Each trace is a computer accumulation of 2500 pulses.

sistent with those reported by McLean and Sauer [35] of two different triplet formation mechanisms in reduced and unreduced PS-I reaction center of spinach.

To account for the present observations in *Mastigocladus*, we consider the primary event in terms of process [3] and the models suggested previously for the blocked and unbloked systems [20,35,38,39]:

(a) In the unblocked system the electron-transfer process is represented by:

$$\begin{array}{ccc} P^*\text{-}700A_1A_2 & \longrightarrow & [\dot{P}^+\text{-}700\dot{A}^1]^sA_2 \\ \uparrow h\nu & & \downarrow \\ P\text{-}700\,A_1A_1 & \xleftarrow{\approx 100\ ms} \cdots \leftarrow & [\dot{P}^+\text{-}700A_1]\dot{A}_2^- \end{array} \qquad (7)$$

When the cycle in Eqn. 7 has been light-initiated and initial charge separation achieved, the electron-transport chain is decoupled from the antenna for approx. 100 ms, allowing the cycle to complete [20,35,38,39]. As only ground-state neutral species qualify for promotion to an excited state [22], two possible Chl *a*, in two different chemical environments, are eligible for photoexcitation:

(i) Chl $a_{antenna}$, which now can be promoted to its triplet state via:

$$Chl\ a_{antenna} \xrightarrow{h\nu} Chl\ a^*_{antenna} \xrightarrow[antenna]{\text{spin orbit intersystem crossing}} Chl\ a^T_{antenna} \qquad (8)$$

and

(ii) A_1, in the electron-transport chain, rapidly transfers its charge and becomes available:

$$\dot{P}^+\text{-}700\,\dot{A}_1^-A_2 \xrightarrow{<1\,\mu s} \dot{P}^+\text{-}700A_1\dot{A}_2^- \xrightarrow{h\nu} \dot{P}^+\text{-}700A_1^*\dot{A}_2^- \xrightarrow{\text{spin orbit intersystem crossing}} \dot{P}^+\text{-}700A_1^T\dot{A}_2^- \qquad (9)$$

The EPR triplet spectrum obtained in this system (Fig. 4, spectrum I) displays polarization patterns indicative of spin orbit intersystem crossing. The zero-field splitting parameters are very similar to Chl a^T in in vitro preparations and those obtained for P^T-700 (cf. Table I). The kinetic behaviour measured at the canonical orientations (given in Fig. 5) display a lifetime of approx. 2 ms, again typical of in vitro Chl *a* [36,37].

Since the ratio of Chl $a_{antenna}$ to A_1 is of the order of 50 : 1 one might assume that the spin orbit intersystem crossing triplet observed in this system arises from the antenna for concentration reasons. On the other hand a recent paper [35] reports a spin orbit intersystem crossing triplet spectrum in a spinach preparation exhibiting a $|D|$ value of 0.0301 cm^{-1}, substantially larger than the one reported here. Nevertheless, the $|D|$ value of that spinach sample when blocked is identical with ours (cf. Table I). This might indicate that the Chl a^T reported here resides in a chemical environment similar to the P^T-700 and would thus be A_1^T.

(b) In the blocked system (A_2 and further electron acceptors are reduced prior to photoexcitation):

$$\begin{array}{ccc} P^*\text{-}700A_1\dot{A}_2^- & \longrightarrow & [\dot{P}^+\text{-}700\dot{A}_1^-]^S\dot{A}_2^- \\ \uparrow & & \downarrow \\ h\nu & & [\dot{P}^+\text{-}700\dot{A}_1^-]^T\dot{A}_2^- \\ \vert & & \downarrow \\ P\text{-}700A_1\dot{A}_2^- & \xleftarrow{\approx 1\ ms.} & [P^T\text{-}700A_1]\dot{A}_2^- \end{array} \qquad (10)$$

Electron transfer cannot proceed beyond the initial radical pair $[\dot{P}^+\text{-}700\dot{A}_1^-]^T$ having triplet character (scheme 10). The paths open for the complex

TABLE I

ZERO-FIELD SPLITTING PARAMETERS OF Chl *a* IN VARIOUS MEDIA

Medium	$\|D\|$ [a]	$\|E\|$ [a]	Method	Reference
n-octane	0.0280	0.0038	ODMR	40
ethanol	0.0262	0.0032	EPR	41
MTHF	0.0281	0.0039	EPR	42
pyr-tol	+0.0273 [b]	−0.0040 [b]	EPR	43
ethanol	0.0274	0.0032	EPR	44
PS-I reaction center [c]	0.0283	0.0040	EPR	22
PS-II reaction center	0.0290	0.0044	EPR	22
PS-I reaction center [c]	0.0278	0.0038	EPR	35
PS-I reaction center [d]	0.0301	0.0039	EPR	35
PS-I reaction center [d,e]	0.0283 [f]	0.0040 [f]	EPR	this work
PS-I reaction center [c,e]	0.0274 [g]	0.0043 [g]	EPR	this work

[a] In cm^{-1}, accurate to ± 0.0005.
[b] Real signed D, E values.
[c] Blocked system.
[d] Unblocked system.
[e] For the exact sample composition, see experimental in the main text.
[f] Extracted from Fig. 4, spectrum I.
[g] Extracted from Fig. 4, spectrum II.

are then a back electron transfer in the radical pair to form P^T-700 in the radical pair intersystem crossing mechanism (Eqs. 3 and 10), or a charge recombination and decay back to the initial singlet ground state. The fact that the triplet spectrum in the blocked system is still observed indicates that the rates in the reaction (Eqn. 11) are:

$$[\dot{P}^+\text{-}700\dot{A}_1^-]^S\dot{A}_2^- \rightarrow [\dot{P}^+\text{-}700\dot{A}_1^-]^T\dot{A}_2^- \rightarrow [P^T\text{-}700A_1]\dot{A}_2^- \quad (11)$$

fast enough to compete with the back reaction to the ground singlet, and are thus in the sub-microsecond time scale. Further, it is seen that once the triplet state has been created in the radical pair intersystem crossing mechanism, it does not have a typical in vitro Chl *a* lifetime, although it does exhibit the same $|D|$ and $|E|$ zero-field splitting parameters (cf. Table I and Fig. 6). This implies that this Chl *a* resides in a different chemical environment and is attributed to P^T-700. This different environment is responsible for the observed lifetime shortening. The blocked cycle time is reduced to approx. 1 ms as compared to 100 ms in in the unblocked system. This explains why Chl $a^T_{antenna}$ (reaction 8) or A_1^T formed by the following reaction:

$$[P^T\text{-}700A_1]\dot{A}_2^- \xrightarrow{h\nu} [P^T\text{-}700A_1^*]\dot{A}_2^- \xrightarrow{\text{spin orbit intersystem crossing}} [P^T\text{-}700A_1^T]\dot{A}_2^- \quad (12)$$

are not observed (cf. Fig. 4, spectrum II vs. I). As the system cycle time is reduced a 100-fold the photoexcited triplet yield, A_1^T and Chl $a^T_{antenna}$ would diminish accordingly, and their steady state concentration is beyond the detection limit.

In a recent paper [22] a study of PS-I reaction center of spinach, in which the A_2 acceptor and the rest of the iron-sulfur centers have been removed, is reported. There again the triplet spectrum is attributed to radical pair intersystem crossing mechanism, whereas that due to spin orbit intersystem crossing could not be observed. This result can be explained in the framework outlined above. As nothing can accept the charge from A_1^- it cannot be photoexcited to the triplet state and the most that system could do is loop in reaction path [10].

Conclusion

In this work we demonstrate that in *Mastigocladus*, PS-I reaction center known to have the minimal subunit structure of higher plant type, the primary photochemical processes are identical to the most evolved systems, namely spinach PS-I reaction center. Employing light modulation EPR spectroscopy enables one to determine the mechanism in which the photoexcited triplet in *Mastigocladus* PS-I reaction center is being formed, namely conventional spin orbit or radical pair intersystem crossing. The triplet EPR spectrum originating in both mechanisms is of the same chemical entity namely Chl *a* as determined from the zero-field splitting parameters $|D|$ and $|E|$. However, the different kinetic behavior associated with each spectrum indicates that these Chl *a* reside in different chemical environments. It is also shown that although light modulation EPR spectroscopy is a relatively slow method in the time scale of the primary photoevents, a substantial amount of information on the fate of the primary processes can be drawn from it. In addition, comparison of the EPR spectra of the bound ferredoxins of the four subunit PS-I reaction center of *Mastigocladus* with that of the seven subunit spinach leads to the conclusion that they are similar in the iron-sulfur centers content.

Acknowledgements

The research described herein was supported by a grant of the Israel Academy for Sciences and Humanities (H.L.). The Fritz Haber Research Center is supported by the Minerva Gesellschaft für die Förschung GmbH, München, F.R.G. This work is in partial fulfillment of the requirements for a Ph.D. degree at the Hebrew University of Jerusalem (O.G.).

References

1 Bengis, C. and Nelson, N. (1975) J. Biol. Chem. 250, 2783–2788
2 Bengis, C. and Nelson, N. (1977) J. Biol. Chem, 252, 4564–4569
3 Nelson, N. and Notsani, B. (1977) in Bioenergetics of Membranes (Packer, L., Papageorgiou, G.C. and Trebst, A., eds.), pp. 234–244, Elsevier, Amsterdam
4 Nechushtai, R., Nelson, N., Mattoo, A.K. and Edelman, M. (1981) FEBS Lett. 125, 115–119
5 Nechushtai, R. and Nelson, N. (1981) J. Biol. Chem. 256, 11624–11628
6 Takahashi, Y. and Katoh, S. (1983) Arch. Biochem. Biophys. 219, 219–227
7 Nechushtai, R., Muster, P., Binder, A., Liveanu, V. and Nelson, N. (1983) Proc. Natl. Acad. Sci. USA 80, 1179–1183
8 Kok, B. (1961) Biochim. Biophys. Acta. 48, 527–533
9 Shuvalov, V.A., Dolan, E. and Ke, B. (1979) Proc. Natl. Acad. Sci. USA, 76, 770–773
10 Heathcote, P., Timofeev, K.N. and Evans, M.C.W. (1979)N FEBS Lett. 101, 105–109
11 Bonnerjea, J. and Evans, M.C.W. (1982) FEBS Lett. 148, 313–316
12 Malkin, R. (1982) Annu. Rev. Plant Phys. 33, 455–479
13 Malkin, R. and Bearden, A.J. (1971) Proc. Natl. Acad. Sci. USA. 68, 16–19
14 Evans, M.C.W., Telfer, A. and Lord, A.V. (1972) Biochim. Biophys. Acta 267, 530–537
15 Evans, M.C.W. and Cammack, R. (1975) Biochim. Biophys. Res. Commun. 63, 187–193
16 Cammuck, E.H. and Evans, M.C.W. (1976) Biochim. Biophys. Res. Commun. 68, 1212–1218
17 Malkin, R., Bearden, A.J. Hunter, F.A. Alberte, R.S. and Thornber, J.P. (1976) Biochim. Biophys. Acta 430, 389–394
18 McIntosh, A.R. and Bolton, J.R. (1976) Biochim. Biophys. Acta. 430, 555–559
19 Evans, E.H., Dickson, D.P.E., Johnson, C.E., Rush, J.D. and Evans, M.C.W. (1981) Eur. J. Biochem. 118, 81–84
20 Gast, P., Swarthoff, T., Ebskamp F.C.R. and Hoff, A.J. (1983) Biochim. Biophys. Acta, 722, 163–175
21 Nelson, N., Bengis, C., Silver, B.L., Getz, D. and Evans, M.C.W. (1975) FEBS Lett. 58, 363–365
22 Rutherford, A.W. and Mullet, J.E. (1981) Biochim. Biophys. Acta. 635, 225–235
23 Levanon, H. and Norris, J.R. (1982) Molecular Biology and Biophysics, Vol. 35, Light Reaction Path of Photosynthesis (Francis K. Fong, ed.), pp. 155–195, Springer-Verlag, Berlin
24 Levanon, H. and Norris, J.R. (1978) Chem. Rev. 18, 185–198
25 Thurnauer, M.C. (1979) Rev. Chem. Int. 3, 197–229
26 Frank, H.A., Bolt, J., Friesner, R. and Sauer, K. Biochim. Biophys. Acta (1979) 547, 502–511
27 Frank, H.A., Friesner, R., Nairn, J.A., Dismukes, C. and Sauer, K. (1979) Biochim. Biophys. Acta 547, 484–501
28 Thurnauer, M.C., Katz, J.J. and Norris, J.R. (1975) Proc. Natl. Acad. Sci. USA 72, 3270–3274
29 Arnon, D.I. (1949) Plant Physiol. 24, 1–15
30 Douglas, M. and Butow, R.A. (1979) Proc. Natl. Acad. Sci. USA 1083–1086
31 Castenholz, R.W. (1969) J. Phycol. 5, 360–368
32 Binder, A., Locher, P. and Zuber, H. (1972) Arch. Hydrobiol. 70, 514–545
33 Binder, A. and Bachofen, R. (1979) FEBS Lett. 104, 66–70
34 Levanon, H. (1979) in Multiple Electronic Resonance (Dorio, M. and Freed, J.H., eds.), Ch. 13, Plenum Press, New York
35 McLean, M.B. and Sauer, K. (1982) Biochim. Biophys. Acta, 679, 384–392

36 Nissani, E., Scherz, A. and Levanon, H. (1977) Photochem. Photobiol. 25, 93–101
37 Levanon, H. and Scherz, A. (1975) Chem. Phys. Lett. 31, 119–124
38 Dismukes, D.C., McGuire, A., Blankenship, R. and Sauer, K. (1978) Biophys. J. 21, 239–256
39 Sauer, K., Mathis, P., Acker, S. and Van Best, J.A. (1978) Biophys. Biochim. Acta 503, 120–134
40 Kleibeuker, J.F., Platenkamp, R.J. and Schaafsma, T.J. (1975) Chem. Phys. Letters, 41, 557–561
41 Levanon, H. and Grebel, V. (1980) Chem. Phys. Letters, 72, 218–224
42 Kleibeuker, J.F. and Schaafsma, T.J. (1974), Chem. Phys. Letters, 29, 116–122
43 Thurnauer, M.C. and Norris, J.R. (1977) Chem. Phys. Letters, 47, 100–105
44 Norris, J.R., Uphaus, R.A. and Katz, J.J. (1975) Chem. Phys. Lett. 31, 157–161